

AUTO-SECONDARIES ON A MIDSIZE ICY MOON: BRIGHT RAYED CRATER INKTOMI (RHEA).

P. Schenk¹, T. Hoogenboom¹ and M. Kirchoff², ¹Lunar & Planetary Institute, Houston TX (schenk@lpi.usra.edu), ²Southwest Research Institute, Boulder, CO.

Introduction: Recent mapping and studies of small craters superposed on large young craters on the Moon [1, 2] point to a growing awareness that secondary craters can form within the ejecta deposit and on the floors of the primary source crater itself. These “self-secondaries” (or auto-secondaries) may be an important and underappreciated phenomenon in cratering that could contaminate primary cratering records and alter interpretations of the ages of young surfaces [3]. In this report we describe small craters formed on the floor of Inktomi, a very recently formed rayed impact crater on Saturn’s midsize icy moon Rhea. These craters may constitute an unusually prominent and well-documented set of auto-secondaries on a planetary surface.

Inktomi Crater: Cassini global mapping of Rhea revealed a prominent bright ray system centered on the fresh 48-km-wide complex crater Inktomi. The bright rays from Inktomi radiate up to ~700 km from crater center and is the most prominent on any of the Saturnian satellites, indicating that Inktomi is the youngest impact crater larger than 10 km in the Saturn system. Cassini targeted three sets of high-resolution images over Inktomi.

Inktomi formed in rugged heavily cratered terrain. The rim of Inktomi is a continuous inward-facing scarp ~3 km high. Floor materials are characterized by numerous interlaced sinuous ridges and scarps. These ridges and scarps grade into a central peak complex ~12 km wide and ~2 km high. A few debris slides are evident along the base of the rim scarp. A mantling, sculpted ejecta deposit surrounds Inktomi to approximately one crater diameter from the crater rim (Fig. 1). The rare post-Inktomi craters within the ejecta deposits have an average areal density of ~1 crater per 10 km².

Surrounding Inktomi we identify fields of smaller clustered craters (Fig. 1). These distinctive craters are found in an annular zone ~1 crater diameter from the rim and beyond, and are always associated with the bright ray deposits of Inktomi. They are interpreted as secondary craters, and demonstrate that secondary craters do in fact form on lower gravity bodies. Further, stereo images of this western portion of this secondary field show that these irregular craters form preferentially on Inktomi-facing slopes.

High-resolution images of the floor and eastern ejecta deposit of Inktomi (Fig. 2) reveal hundreds of small craters concentrated along the central eastern crater floor and the central eastern sector of the ejecta deposit at Inktomi. These clustered craters do not occur within the concentric zone exterior to the main

ejecta deposit, but in a crudely oval zone from the secondary field inner limit all the way to the eastern flanks of the central peak of Inktomi (Fig. 2). The western half and the southern and northern thirds of the crater floor are essentially crater-free at this resolution, consistent with an extremely young age for Inktomi. The dense concentration of small craters in a tightly restricted area on the floor of a large extremely young impact crater is thus highly unusual.

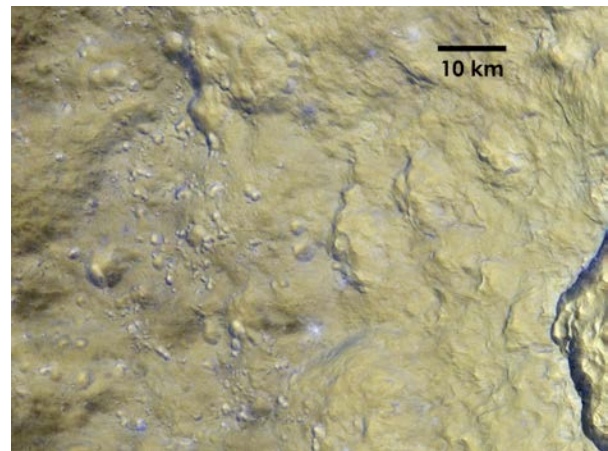


Figure 1. Crop of s49 color mosaic showing western quadrant of Inktomi ejecta and secondary field. Inktomi rim is at far right, surrounded by deeply rolling terrain mantled by ejecta. Discrete secondary craters are visible in left third of image, highlighted by irregular shapes and strong brightness contrast. A small post-Inktomi bright ray crater is visible at lower center.

The eastern Inktomi craters are distinct for their tight spatial clustering and narrow size distribution (Fig. 3) and resemble secondary craters. No mechanism is known by which a swarm of hundreds of projectiles could have produced such a tight cluster on such a young surface after the impact itself.

Crater counts of definable secondary craters in the western sector (Fig. 3) show that these craters have a SFD different from selected typical heavily cratered areas on Rhea [4] (Fig. 3). Craters throughout the outer secondary crater fields at Inktomi average ~1 km +/- 0.5 km (Fig. 3) with the largest ~2.5 km across. This puts the maximum crater size within the canonical secondary crater field at ~0.05D_{Inktomi}, broadly consistent with the lunar rule [5] and with known secondaries on Europa [6]. Craters on both the floor and eastern ejecta deposit of Inktomi peak at a mean of ~400 m diame-

ter (Fig. 3). This is approximately half the size of the classical secondaries observed in the western sector of the secondary field.

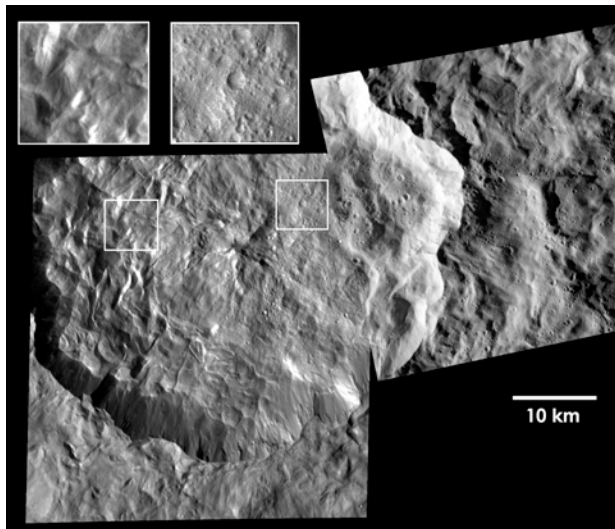


Figure 2. Two frame mosaic of 35-m pixel scale images over the floor and eastern ejecta sector of Inktomi crater. Insets show details of contrasting small crater density on western floor (left box) and eastern floor (right box) (north is to top).

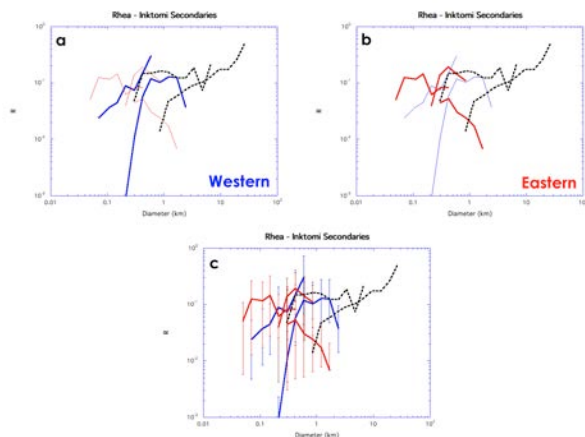


Figure 4. Crater size-frequency R-plots of crater counts associated with Inktomi crater.

The maximum size of craters in the eastern floor and ejecta is ~ 1.5 km, which would require a primary source crater at least 25 km across. The next largest rayed craters on Rhea are only 7 km wide [7], less than $1/5^{\text{th}}$ the diameter of Inktomi and capable of producing secondaries not much larger than ~ 350 m. No fresh (rayed or not) craters > 5 km have been identified within 100 km of Inktomi. Thus, there are no other large craters on Rhea younger than Inktomi capable of pro-

ducing these clustered craters on the floor of Inktomi. The only source of large numbers of small craters of this size is Inktomi itself, and we conclude that these floor craters formed by fall-back of secondary ejecta blocks on near vertical trajectories.

The mechanism responsible for auto-secondaries is not yet clear [2], but early phase vertical jetting is one suspect. The cluster of floor craters is on the eastern quadrant of Inktomi, which is also direction in which the ray patterns are shortest and the inferred direction of oblique impact. Whether the formation of auto-secondaries is linked to oblique impact is unclear from this single example but may be demonstrated by future mapping on other planets.

Discussion: Inktomi represents an extreme and concentrated example of what may be a significant Solar System wide cratering process; namely, auto-secondaries (or self-secondary) cratering. Mapping of small craters shows factors of 4 or more difference in crater density on adjacent terrains and within terrains proximal to recent large lunar craters [1, 2]. Auto-secondaries therefore represent a potentially significant contributor to the mapped small crater populations on recently resurfaced crater floors and ejecta deposits, potentially compromising efforts to date the ages of these events [3]. Other examples of large fresh craters with secondaries include Sagaris (D ~ 48 km) and Sabinus (D ~ 88 km) on Dione and Telamachus (D ~ 93 km) on Tethys and Yu-ti (D ~ 67 km) on Rhea. Auto-secondaries have not been observed on these craters, but we note that they were not observable at Inktomi until pixel resolutions were better than ~ 200 m, which is the best available imaging for any of the examples cited above. Efforts to map similar such craters on other bodies will require adequate resolution. Efforts to determine the ages of such recent craters must consider potential auto-secondary contamination through detailed examination of the spatial density variability across the entire crater floor and ejecta deposit. Minimization of the effects of possible auto-secondary contamination includes use of the entire crater floor and ejecta as a counting surface to reduce the amount of auto-secondaries included, and quotation of ages as maximum ages due to the potential presence of non-primary post-impact cratering.

References: [1] Zanetti, M. et al., (2015) Lunar Planet. Sci. Conf 46, 1209; [2] Plescia, J. et al., (2015) Lunar Planet. Sci. Conf 46, 2535; [3] Hiesinger, H., et al. (2012) *J. Geophys. Res.*, 10.1029/2011JE003935; [4] Kirchoff, M. and P. Schenk (2010) *Icarus* **206**, 485; [5] Allen, C. (1979) *Geophys. Res. Lett.* **6**, 51; [6] Singer, K., W. McKinnon, and L. Nowicki (2013) *Icarus* **226**, 865; [7] Schenk, P., and S. Murphy (2011) Lunar Planet. Sci. Conf 42, 2098.